Reconstruction of Permittivity Profiles in Cylindrical Objects Illuminated by Higher Order TE_{mn} and TM_{mn} Modes

M. J. Akhtar, *Student Member, IEEE,* and Abbas S. Omar, *Senior Member, IEEE*

***Abstract*—An improved and accurate technique for the reconstruction of radially dependent permittivity profiles in cylindrical objects illuminated by higher order TE_{mn} and TM_{mn} cylindrical modes is presented in this paper. The technique is based on a general kind of integral transform of the measured frequency-dependent reflection data and the recently suggested renormalization technique to obtain a unique solution of the corresponding inverse problem. Nonlinear Riccati-similar differential equations for a properly defined reflection coefficient for both TE_{mn} and TM_{mn} cylindrical modes have first been derived in a unified way for this purpose. These equations have then been inverted using our proposed renormalization technique to uniquely obtain the unknown permittivity profile in terms of a Hankel transform of measured reflection coefficient data. About 150–200 measurement data points over a wide frequency band (wavelength ranging from one-fifth of the inner diameter of the cylindrical object to infinity) have been used for the reconstruction. A dummy time variable has been introduced to improve the overall reconstruction process. This variable has then been transformed into the spatial one with the help of a proposed numerical algorithm. A number of reconstruction examples has been considered and a very good agreement has been found between the original and reconstructed profiles even for very high values of permittivity.**

***Index Terms*—Biomedical electromagnetic imaging, electromagnetic scattering inverse problems, microwave imaging, remote sensing, tomography.**

I. Introduction

RECONSTRUCTION of permittivity profiles in a cylindrical coordinate system plays a very significant role in a number of research areas because of its wide variety of practical applications. Some of the applications include, e.g., environmental studies of water content, aging and possible diseases of trees in forests (e.g., [1], [2]), earth structure as seen from an exploration well in oil fields [3], and imaging of human organs in biomedical microwave tomography [4], [5]. Generally, most of the methods reported in the literature for the profile reconstruction employ a source reconstruction philosophy in either spectral or spatial domain, leading to a nonunique and uncertain solution of the corresponding nonlinear inverse problem (e.g., [5], [6]). A unique solution may be obtained only when the so-called "Born approximation" is used [7]. However, only objects with very low permittivity can be reconstructed using this approximation.

An alternative approach for reconstructing the permittivity profiles in planar structures is the Riccati differential-equation technique [8], which has been improved and combined with "renormalization techniques" in recent years to cover objects with higher profile's contrasts [9], [10]. The main advantage of this method is its quasi-linearity, which leads to a unique solution. We recently applied this approach to reconstruct the radially dependent permittivity profiles in cylindrical objects with TM_{00} illumination, which represents an axially and azimuthally independent incident wave [11]. As exciting and receiving cylindrical modes with high modal purity (e.g., TM_{00}) are generally not feasible in most of the practical cases, reconstruction of the permittivity profile making use of a mixed-mode illumination is recommended.

This paper consists of two parts. The first part deals with the formulation of the direct problem. Nonlinear Riccati-similar differential equations for an appropriately defined reflection coefficient for the higher order TE_{mn} and TM_{mn} cylindrical modes have been derived in a unique way for this purpose. These nonlinear equations have next been solved using MATLAB to generate synthetic reflection coefficient data for a known permittivity profile. The overall formulation is quite general and can be used for all types of cylindrical structures having outside illumination.

In the second part of this paper, the derived nonlinear Riccati-similar equations have been inverted using our proposed renormalization technique and a general kind of integral transform of the measured scattering data, which leads to a unique reconstruction of the permittivity profile. It may be noted here that because of the azimuthal dependence of the propagation constants of these higher order modes, the solution of the inverse problem becomes a tedious process. The main problem lies in the separation of the frequency and space dependences of the radial propagation constant. We have introduced here the concept of effective relative permittivity to tackle this problem. Various parameters are adjusted to optimize the value of this effective relative permittivity. A dummy time variable has been introduced as well in order to improve the overall reconstruction process. Accordingly, a numerical algorithm has been proposed to reconstruct the profile in the real space domain from this virtual time variable. A number of reconstruction examples has been considered in Section IV.

Manuscript received March 5, 2000; revised August 25, 2000. This work was supported by the Deutsche Forschungsgemeinschaft under Grant DFG OM 4 /16-1.

The authors are with Chair of Microwave and Communication Engineering, FET-IESK, University of Magdeburg, 39016 Magdeburg, Germany.

Publisher Item Identifier S 0018-9480(00)10752-5.

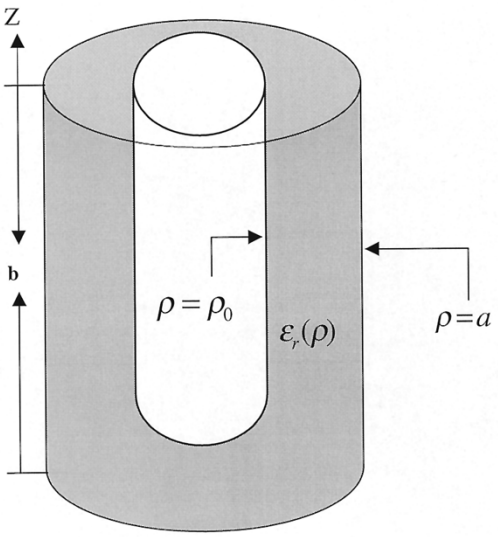

Fig. 1. Radially varying permittivity profile.

II. Formulation of the Direct Problem

Let us consider a cylindrical dielectric object of the outer radius a, the inner radius ρ_0, and a radially varying permittivity profile $\varepsilon_r(\rho)$, as shown in Fig. 1. The object is located between two conducting plates at $z=0$ and $z=b$ and illuminated by a higher order cylindrical mode of either TE_{mn} or TM_{mn} polarized wave of wavenumber k_0 from the outer free space ($\rho>a$). The radial propagation constant is azimuthally and axially dependent for these higher order modes as compared to that of the TM_{00} case [11]. The reflection coefficient is measured at the outer radius of the cylindrical body to comply with most practical cases and, thus, the inward and outward traveling waves are treated as being incident and reflected ones, respectively.

A. Riccati-Similar Differential Equations for the TE_{mn} Cylindrical Wave

First, we will consider the TE_{mn} illumination for the analysis. The field components of TE_{mn} cylindrical mode are given by [12]

$$E_\rho^- = \frac{n}{\rho}\sin(k_z z)\sin(n\phi)H_n^{(1)}(k_\rho\rho)$$
$$E_\rho^+ = \frac{n}{\rho}\sin(k_z z)\sin(n\phi)H_n^{(2)}(k_\rho\rho) \quad (1)$$
$$E_\phi^- = k_\rho\sin(k_z z)\cos(n\phi)H_n^{(1)\prime}(k_\rho\rho)$$
$$E_\phi^+ = k_\rho\sin(k_z z)\cos(n\phi)H_n^{(2)\prime}(k_\rho\rho) \quad (2)$$
$$E_z^- = 0 \quad E_z^+ = 0 \quad (3)$$
$$H_\rho^- = \frac{k_z k_\rho}{j\omega\mu_0}\cos(k_z z)\cos(n\phi)H_n^{(1)\prime}(k_\rho\rho)$$
$$H_\rho^+ = \frac{k_z k_\rho}{j\omega\mu_0}\cos(k_z z)\cos(n\phi)H_n^{(2)\prime}(k_\rho\rho) \quad (4)$$
$$H_\phi^- = \frac{-nk_z}{j\omega\mu_0\rho}\cos(k_z z)\sin(n\phi)H_n^{(1)}(k_\rho\rho)$$
$$H_\phi^+ = \frac{-nk_z}{j\omega\mu_0\rho}\cos(k_z z)\sin(n\phi)H_n^{(2)}(k_\rho\rho) \quad (5)$$
$$H_z^- = \frac{k_\rho^2}{j\omega\mu_0}\sin(k_z z)\cos(n\phi)H_n^{(1)}(k_\rho\rho)$$
$$H_z^+ = \frac{k_\rho^2}{j\omega\mu_0}\sin(k_z z)\cos(n\phi)H_n^{(2)}(k_\rho\rho) \quad (6)$$

where the "$-$" and "$+$" signs represent inward and outward propagating waves, respectively, $H_n^{(p)}(k_\rho\rho)$ is the Hankel function of pth type and nth order, $H_n^{(p)\prime}(k_\rho\rho)$ is the first derivative of the corresponding Hankel function,

$$k_\rho = \sqrt{k^2 - k_z^2} = \sqrt{k_0^2\varepsilon_r(\rho) - \left(\frac{m\pi}{b}\right)^2} \quad (7)$$

is the radial propagation constant, and $k_z = (m\pi/b)$ is the propagation constant in the axial direction.

We are looking for a taper solution of the form

$$H_z = H_z^- + \tilde{\Gamma}H_z^+ = H_z^- - \tilde{\Gamma}(H_z^-)^* \quad (8)$$
$$E_\phi = E_\phi^- + \tilde{\Gamma}E_\phi^+ = E_\phi^- + \tilde{\Gamma}(E_\phi^-)^* \quad (9)$$

where $\tilde{\Gamma}$ is an appropriately defined reflection coefficient and "*" denotes the complex conjugate.

We now define

$$Z = -\frac{E_\phi^-}{H_z^-} = -\frac{jk_0Z_0}{k_\rho}\frac{H_n^{(1)\prime}(k_\rho\rho)}{H_n^{(1)}(k_\rho\rho)} \quad (10)$$

and

$$\alpha = \frac{Z^*}{Z} = -\frac{H_{n-1}^{(2)}(k_\rho\rho) - H_{n+1}^{(2)}(k_\rho\rho)}{H_{n-1}^{(1)}(k_\rho\rho) - H_{n+1}^{(1)}(k_\rho\rho)}\frac{H_n^{(1)}(k_\rho\rho)}{H_n^{(2)}(k_\rho\rho)} \quad (11)$$

where Z_0 is the free-space intrinsic impedance.

Equations (8)–(11) can be combined together to obtain

$$H_z = H_z^-(1+\Gamma) \quad E_\phi = -ZH_z^-(1-\alpha\Gamma) \quad (12)$$

where

$$\Gamma = -\tilde{\Gamma}\frac{(H_z^-)^*}{H_z^-}. \quad (13)$$

Next, we rewrite Maxwell's equations for a TE_{mn} mode to obtain the following forms:

$$\frac{\partial H_z}{\partial\rho} = -\frac{jk_\rho^2}{\omega\mu_0}E_\phi$$
$$\frac{\partial}{\partial\rho}(\rho E_\phi) = j\omega\mu_0\rho\left(\frac{n^2}{\rho^2k_\rho^2} - 1\right)H_z. \quad (14)$$

From (12)–(14), we arrive at

$$\frac{\partial}{\partial\rho}[(1+\Gamma)H_z^-] = \frac{jk_\rho^2}{k_0}\overline{Z}(1-\alpha\Gamma)H_z^- \quad (15)$$
$$\frac{\partial}{\partial\rho}[\rho\overline{Z}(1-\alpha\Gamma)H_z^-] = jk_0\rho\left(1 - \frac{n^2}{\rho^2k_\rho^2}\right)(1+\Gamma)H_z^- \quad (16)$$

where

$$\overline{Z} = \frac{Z}{Z_0} = -\frac{jk_0}{k_\rho}\frac{H_n^{(1)'}(k_\rho\rho)}{H_n^{(1)}(k_\rho\rho)} = -\frac{jk_0}{2k_\rho}\left[\frac{H_{n-1}^{(1)}(k_\rho\rho)}{H_n^{(1)}(k_\rho\rho)} - \frac{H_{n+1}^{(1)}(k_\rho\rho)}{H_n^{(1)}(k_\rho\rho)}\right] \tag{17}$$

is a normalized local impedance. Next, (15) and (16) are solved simultaneously to eliminate H_z^- and to arrive at the nonlinear differential equation for Γ, shown in (18), at the bottom of this page.

Equation (18) can be simplified using (11) and (17) to have the form of (19), shown at the bottom of this page, which is a nonlinear Riccati-similar differential equation for the radially (and frequency) dependent reflection coefficient $\Gamma(k_0, \rho)$ due to a higher order TE_{mn} illumination.

B. Riccati-Similar Differential Equation for the TM_{mn} *Cylindrical Wave*

The analysis for the TM_{mn} illumination is done in a similar way as for the TE_{mn} illumination. The electromagnetic-field components for this mode are given by [12]

$$E_\rho^- = \frac{k_z k_\rho}{j\omega\varepsilon}\sin(k_z z)\cos(n\phi)H_n^{(1)'}(k_\rho\rho)$$
$$E_\rho^+ = \frac{k_z k_\rho}{j\omega\varepsilon}\sin(k_z z)\cos(n\phi)H_n^{(2)'}(k_\rho\rho) \tag{20}$$
$$E_\phi^- = \frac{nk_z}{j\omega\varepsilon\rho}\sin(k_z z)\sin(n\phi)H_n^{(1)}(k_\rho\rho)$$
$$E_\phi^+ = \frac{nk_z}{j\omega\varepsilon\rho}\sin(k_z z)\sin(n\phi)H_n^{(2)}(k_\rho\rho) \tag{21}$$
$$E_z^- = \frac{k_\rho^2}{j\omega\varepsilon}\cos(k_z z)\cos(n\phi)H_n^{(1)}(k_\rho\rho)$$
$$E_z^+ = \frac{k_\rho^2}{j\omega\varepsilon}\cos(k_z z)\cos(n\phi)H_n^{(2)}(k_\rho\rho) \tag{22}$$

$$H_\rho^- = -\frac{n}{\rho}\cos(k_z z)\sin(n\phi)H_n^{(1)}(k_\rho\rho)$$
$$H_\rho^+ = -\frac{n}{\rho}\cos(k_z z)\sin(n\phi)H_n^{(2)}(k_\rho\rho) \tag{23}$$
$$H_\phi^- = -k_\rho\cos(k_z z)\cos(n\phi)H_n^{(1)'}(k_\rho\rho)$$
$$H_\phi^+ = -k_\rho\cos(k_z z)\cos(n\phi)H_n^{(1)'}(k_\rho\rho) \tag{24}$$
$$H_z^- = 0 \quad H_z^+ = 0 \tag{25}$$

where $\varepsilon = \varepsilon_0\varepsilon_r(\rho)$ is the permittivity in the dielectric medium and the other symbols have the same meaning as in the TE_{mn} case.

Here, we are looking for a taper solution of the form

$$E_z = E_z^- + \tilde{\Gamma}E_z^+ = E_z^- - \tilde{\Gamma}(E_z^-)^* \tag{26}$$
$$H_\phi = H_\phi^- + \tilde{\Gamma}H_\phi^+ = H_\phi^- + \tilde{\Gamma}(H_\phi^-)^*. \tag{27}$$

Next, we define

$$Y = \frac{H_\phi^-}{E_z^-} = -\frac{jk_0Y_0\varepsilon_r(\rho)}{k_\rho}\frac{H_n^{(1)'}(k_\rho\rho)}{H_n^{(1)}(k_\rho\rho)} \tag{28}$$

where Y_0 is the free-space intrinsic admittance.

The following points may be noted here: 1) the field components considered in the TM_{mn} case are E_z and H_ϕ [see (26) and (27)], which is complementary to the TE_{mn} case, where H_z and E_ϕ (12) are considered and 2) the admittance Y is considered for analysis in the TM_{mn} case, whereas in the TE_{mn} case, the impedance Z is considered. The reason is that the field components involving the derivative of Hankel functions are always taken in the numerator in order to simplify the overall analysis.

Next, (26)–(28) can be combined to obtain

$$E_z = E_z^-(1+\Gamma) \quad H_\phi = YE_z^-(1-\alpha\Gamma) \tag{29}$$

where

$$\Gamma = -\tilde{\Gamma}\frac{(E_z^-)^*}{E_z^-} \quad \alpha = \frac{Y^*}{Y} \quad Y = \frac{H_\phi^-}{E_z^-}. \tag{30}$$

$$\frac{\partial\Gamma}{\partial\rho} + \frac{1}{(1+\alpha)\rho\overline{Z}}\left\{\begin{array}{l}\Gamma^2\left[jk_0\rho\left(1-\dfrac{n^2}{\rho^2k_\rho^2}\right) + \dfrac{\partial}{\partial\rho}(\rho\alpha\overline{Z}) - \dfrac{jk_\rho^2}{k_0}\rho\alpha^2\overline{Z}^2\right] \\ +\Gamma\left[2jk_0\rho\left(1-\dfrac{n^2}{\rho^2k_\rho^2}\right) + \dfrac{\partial}{\partial\rho}(\rho(\alpha-1)\overline{Z}) + 2\dfrac{jk_\rho^2}{k_0}\rho\alpha\overline{Z}^2\right] \\ +\left[jk_0\rho\left(1-\dfrac{n^2}{\rho^2k_\rho^2}\right) - \dfrac{\partial}{\partial\rho}(\rho\overline{Z}) - \dfrac{jk_\rho^2}{k_0}\rho\overline{Z}^2\right]\end{array}\right\} = 0 \tag{18}$$

$$\frac{\partial\Gamma}{\partial\rho} + \Gamma\left\{\frac{4j}{\pi\rho H_n^{(1)}(k_\rho\rho)H_n^{(2)}(k_\rho\rho)} - \frac{j\pi\rho}{8}\left[\begin{array}{c}\left(H_n^{(1)}(k_\rho\rho)H_{n-1}^{(2)}(k_\rho\rho) + H_{n-1}^{(1)}(k_\rho\rho)H_n^{(2)}(k_\rho\rho)\right) \\ -\left(H_n^{(2)}(k_\rho\rho)H_{n+1}^{(1)}(k_\rho\rho) + H_{n+1}^{(2)}(k_\rho\rho)H_n^{(1)}(k_\rho\rho)\right)\end{array}\right]\frac{\partial k_\rho}{\partial\rho}\right\}$$
$$= \left\{\frac{j\pi\rho}{4}H_n^{(2)}(k_\rho\rho)\left[H_{n-1}^{(1)}(k_\rho\rho) - \frac{n}{k_\rho\rho}H_n^{(1)}(k_\rho\rho)\right]\frac{\partial k_\rho}{\partial\rho}\right\}\left[1-\alpha\Gamma^2\right] \tag{19}$$

Now, for a TM_{mn} mode, Maxwell's equations are rewritten as

$$\frac{\partial}{\partial\rho}\left[(1+\Gamma)E_z^-\right] = \frac{jk_\rho^2\overline{Y}}{k_0\varepsilon_r(\rho)}(1-\alpha\Gamma)E_z^- \tag{31}$$

$$\frac{\partial}{\partial\rho}\left[\rho\overline{Y}(1-\alpha\Gamma)E_z^-\right] = jk_0\varepsilon_r(\rho)\rho\left(1-\frac{n^2}{\rho^2k_\rho^2}\right)(1+\Gamma)E_z^- \tag{32}$$

where

$$\begin{aligned}\overline{Y} &= \frac{Y}{Y_0}\\ &= -\frac{jk_0\varepsilon_r(\rho)}{k_\rho}\frac{H_n^{(1)\prime}(k_\rho\rho)}{H_n^{(1)}(k_\rho\rho)}\\ &= -\frac{jk_0\varepsilon_r(\rho)}{2k_\rho}\left[\frac{H_{n-1}^{(1)}(k_\rho\rho)}{H_n^{(1)}(k_\rho\rho)}-\frac{H_{n+1}^{(1)}(k_\rho\rho)}{H_n^{(1)}(k_\rho\rho)}\right]\end{aligned} \tag{33}$$

is a normalized local admittance.

Equations (31) and (32) are now solved simultaneously to eliminate E_z^- and to arrive at the nonlinear differential equation for Γ, shown in (34) at the bottom of this page.

Equation (34) can then be simplified using (29), (30), and (33) to arrive at (35), shown at the bottom of this page, which is a nonlinear Riccati-similar differential equation for the radially (and frequency) dependent reflection coefficient $\Gamma(k_0, \rho)$ due to a higher order TM_{mn} illumination.

III. Inverse Solution

A. TE_{mn} Cylindrical Wave

Generally, in most of the practical cases, α, as defined in (11), can be replaced by its asymptotic value for $k_\rho\rho \to \infty$. Hence, (19) can be rewritten as (36), shown at the bottom of this page.

Following the renormalization technique proposed in [10], a linearized version of (36) describing a virtual reflection coefficient $\hat{\Gamma}(\rho)$ can be defined as (37), shown at the bottom of the next page.

It is worth noting that the second term involving $\hat{\Gamma}$ on the left-hand side of (37) approaches zero if the Hankel functions are replaced by their asymptotic expressions. Hence, this term can be neglected provided that the spatial derivative of the permittivity is not too high. The optimum nonlinear transformation relating the measurable reflection coefficient $\Gamma(\rho)$ to the virtual one $\hat{\Gamma}(\rho)$ is found on similar bases, as in [10] and [11]. Equation

$$\frac{\partial\Gamma}{\partial\rho}+\frac{1}{(1+\alpha)\rho\overline{Y}}\left\{\begin{array}{l}\Gamma^2\left[jk_0\rho\varepsilon_r(\rho)\left(1-\frac{n^2}{\rho^2k_\rho^2}\right)+\frac{\partial}{\partial\rho}(\rho\alpha\overline{Y})-\frac{jk_\rho^2}{k_0\varepsilon_r(\rho)}\rho\alpha^2\overline{Y}^2\right]\\ +\Gamma\left[2jk_0\rho\varepsilon_r(\rho)\left(1-\frac{n^2}{\rho^2k_\rho^2}\right)+\frac{\partial}{\partial\rho}(\rho(\alpha-1)\overline{Y})+2\frac{jk_\rho^2}{k_0\varepsilon_r(\rho)}\rho\alpha\overline{Y}^2\right]\\ +\left[jk_0\rho\varepsilon_r(\rho)\left(1-\frac{n^2}{\rho^2k_\rho^2}\right)-\frac{\partial}{\partial\rho}(\rho\overline{Y})-\frac{jk_\rho^2}{k_0\varepsilon_r(\rho)}\rho\overline{Y}^2\right]\end{array}\right\}=0 \tag{34}$$

$$\frac{\partial\Gamma}{\partial\rho}+\Gamma\left\{\begin{array}{l}\frac{4j}{\pi\rho H_n^{(1)}(k_\rho\rho)H_n^{(2)}(k_\rho\rho)}\\ +\frac{j\pi\rho k_\rho^2}{8\varepsilon_r(\rho)}\left[\begin{array}{l}\left(H_n^{(1)}(k_\rho\rho)H_{n-1}^{(2)}(k_\rho\rho)+H_{n-1}^{(1)}(k_\rho\rho)H_n^{(2)}(k_\rho\rho)\right)\\ -\left(H_n^{(2)}(k_\rho\rho)H_{n+1}^{(1)}(k_\rho\rho)+H_{n+1}^{(2)}(k_\rho\rho)H_n^{(1)}(k_\rho\rho)\right)\end{array}\right]\frac{\partial}{\partial\rho}\left(\frac{\varepsilon_r(\rho)}{k_\rho}\right)\end{array}\right\}$$
$$=\left\{-\frac{j\pi\rho k_\rho^2}{4\varepsilon_r(\rho)}H_n^{(2)}(k_\rho\rho)\left[H_{n-1}^{(1)}(k_\rho\rho)-\frac{n}{k_\rho\rho}H_n^{(1)}(k_\rho\rho)\right]\frac{\partial}{\partial\rho}\left(\frac{\varepsilon_r(\rho)}{k_\rho}\right)\right\}\left[1-\alpha\Gamma^2\right] \tag{35}$$

$$\frac{1}{1-\Gamma^2}\frac{\partial\Gamma}{\partial\rho}+\frac{\Gamma}{1-\Gamma^2}\left\{\begin{array}{l}\frac{4j}{\pi\rho H_n^{(1)}(k_\rho\rho)H_n^{(2)}(k_\rho\rho)}-\frac{j\pi\rho}{8}\\ \left[\begin{array}{l}\left(H_n^{(1)}(k_\rho\rho)H_{n-1}^{(2)}(k_\rho\rho)+H_{n-1}^{(1)}(k_\rho\rho)H_n^{(2)}(k_\rho\rho)\right)\\ -\left(H_n^{(2)}(k_\rho\rho)H_{n+1}^{(1)}(k_\rho\rho)+H_{n+1}^{(2)}(k_\rho\rho)H_n^{(1)}(k_\rho\rho)\right)\end{array}\right]\frac{\partial k_\rho}{\partial\rho}\end{array}\right\}$$
$$=\left\{\frac{j\pi\rho}{4}H_n^{(2)}(k_\rho\rho)\left[H_{n-1}^{(1)}(k_\rho\rho)-\frac{n}{k_\rho\rho}H_n^{(1)}(k_\rho\rho)\right]\frac{\partial k_\rho}{\partial\rho}\right\} \tag{36}$$

(37) can then be integrated resulting in (38), shown at the bottom of this page, where k_ρ, as defined by (7), can be rewritten as

$$k_\rho = k_0\sqrt{\varepsilon_r(\rho) - \delta^2} = k_0\sqrt{\tilde{\varepsilon}_r(\rho)} \tag{39}$$

where $\delta = (m/2\overline{b}\,\overline{k}_0)$, $\tilde{\varepsilon}_r(\rho) = \varepsilon_r(\rho) - \delta^2$ (effective relative permittivity), $\overline{k}_0 = (k_0\rho_0/2\pi) = (\rho_0/\lambda_0)$ (normalized free-space wavenumber), and $\overline{b} = (b/\rho_0)$ (normalized length in axial direction).

The above defined parameter δ depends on the wavenumber $\overline{k}_0$. For a systematic solution of the inverse problem, the parameter δ should be frequency independent, which is not generally true and necessitates introducing some simplifying assumptions. One possibility is to substitute the average value of $\overline{k}_0$ over which the scattering data is measured into δ. It has been observed, however, that the overall reconstruction process is much sensitive to the lower value of $\overline{k}_0$. As a matter of fact, the reconstruction is quite good, if the value of $\overline{k}_0$ in δ is taken as three to four times of the lowest value of the wavenumber at which the measurement is carried out. By considering $\hat{\Gamma}(k_0, \rho_0) = 0$ as a boundary condition, we simplify (38) into (40), shown at the bottom of this page.

Now, let us introduce a virtual time variable t according to

$$t = \rho\sqrt{\tilde{\varepsilon}_r(\rho)}, \qquad \Rightarrow dt = \sqrt{\tilde{\varepsilon}_r(\rho)}\left[1 + \frac{\rho}{2\tilde{\varepsilon}_r(\rho)}\,\frac{d\tilde{\varepsilon}_r(\rho)}{d\rho}\right] d\rho \cong \sqrt{\tilde{\varepsilon}_r(\rho)}\, d\rho. \tag{41}$$

The above approximation is valid provided $d\tilde{\varepsilon}_r(\rho)/d\rho$ is not too large.

From (39)–(41), we get

$$\hat{\Gamma}(k_0, t_a) = \int_{t_a}^{t_0} \left\{ \frac{\pi}{8\tilde{\varepsilon}_r(\rho')\sqrt{\tilde{\varepsilon}_r(\rho')}}\,\frac{d\tilde{\varepsilon}_r(\rho')}{d\rho'} \cdot j\,\frac{\left[nH_n^{(1)}(k_0t') - k_0t'H_{n-1}^{(1)}(k_0t')\right]}{H_n^{(1)}(k_0t_a)} \cdot H_n^{(1)}(k_0t')H_n^{(2)}(k_0t_a) \right\} dt' \tag{42}$$

where use is made of the identity

$$\int_{t_a}^{t'} \left[\frac{4j}{\pi t'' H_n^{(1)}(k_0t'')H_n^{(2)}(k_0t'')}\right] dt'' = \ln\left[\frac{H_n^{(1)}(k_0t')H_n^{(2)}(k_0t_a)}{H_n^{(2)}(k_0t')H_n^{(1)}(k_0t_a)}\right] \tag{43}$$

with

$$t_a = a\sqrt{\tilde{\varepsilon}_r(a)} \quad t_0 = \rho_0\sqrt{\tilde{\varepsilon}_r(\rho_0)}. \tag{44}$$

We now introduce the truncated Hankel transform of $\hat{R}(k_0) = \hat{\Gamma}(k_0, t_a)$ according to

$$\hat{r}(t) = \int_0^{\hat{k}_0} \hat{R}(k_0)J_0(k_0t)k_0\, dk_0 \tag{45}$$

$$\frac{\partial\hat{\Gamma}}{\partial\rho} + \hat{\Gamma}\left\{\frac{4j}{\pi\rho H_n^{(1)}(k_\rho\rho)H_n^{(2)}(k_\rho\rho)} - \frac{j\pi\rho}{8}\left[\begin{array}{c}\left(H_n^{(1)}(k_\rho\rho)H_{n-1}^{(2)}(k_\rho\rho) + H_{n-1}^{(1)}(k_\rho\rho)H_n^{(2)}(k_\rho\rho)\right)\\ -\left(H_n^{(2)}(k_\rho\rho)H_{n+1}^{(1)}(k_\rho\rho) + H_{n+1}^{(2)}(k_\rho\rho)H_n^{(1)}(k_\rho\rho)\right)\end{array}\right]\frac{\partial k_\rho}{\partial\rho}\right\} = \left\{\frac{j\pi\rho}{4}\,H_n^{(2)}(k_\rho\rho)\left[H_{n-1}^{(1)}(k_\rho\rho) - \frac{n}{k_\rho\rho}\,H_n^{(1)}(k_\rho\rho)\right]\frac{\partial k_\rho}{\partial\rho}\right\} \tag{37}$$

$$\hat{\Gamma}(k_0, a) = \hat{\Gamma}(k_0, \rho_0)\exp\left\{-\int_{\rho_0}^{a}\left[\frac{4j}{\pi\rho'' H_n^{(1)}(k_{\rho''}\rho'')H_n^{(2)}(k_{\rho''}\rho'')}\,d\rho''\right]\right\} + \int_a^{\rho_0}\left\{\begin{array}{l}\dfrac{j\pi\rho'}{4}\,H_n^{(2)}(k\rho')\left[\dfrac{n}{k_{\rho'}\rho'}\,H_n^{(1)}(k_{\rho'}\rho') - H_{n-1}^{(1)}(k_{\rho'}\rho')\right]\dfrac{\partial k_\rho}{\partial\rho'}\\ *\exp\left[\displaystyle\int_a^{\rho'}\frac{4j}{\pi\rho'' H_n^{(1)}(k_{\rho''}\rho'')H_n^{(2)}(k_{\rho''}\rho'')}\,d\rho''\right]\end{array}\right\} d\rho' \tag{38}$$

$$\hat{\Gamma}(k_0, a) = \int_a^{\rho_0}\left\{\begin{array}{l}\dfrac{j\pi\rho' k_0}{8\sqrt{\tilde{\varepsilon}_r(\rho')}}\,\dfrac{d\tilde{\varepsilon}_r(\rho')}{d\rho'}\,H_n^{(2)}(k\rho')\left[\dfrac{n}{k_{\rho'}\rho'}\,H_n^{(1)}(k_{\rho'}\rho') - H_{n-1}^{(1)}(k_{\rho'}\rho')\right]\\ \cdot\exp\left[\displaystyle\int_a^{\rho'}\frac{4j}{\pi\rho'' H_n^{(1)}(k_{\rho''}\rho'')H_n^{(2)}(k_{\rho''}\rho'')}\,d\rho''\right]\end{array}\right\} d\rho' \tag{40}$$

where $\hat{k}_0$ is the highest wavenumber at which the reflection coefficient is measured.

Inserting (42) into (45) results in

$$\hat{r}(t) = \int_{t_a}^{t_0} G(\tilde{\varepsilon}_r(t'))K(t, t')\,dt' \tag{46}$$

where

$$G(\tilde{\varepsilon}_r(t')) = \frac{\pi}{8\tilde{\varepsilon}_r(\rho')\sqrt{\tilde{\varepsilon}_r(\rho')}}\frac{d\tilde{\varepsilon}_r(\rho')}{d\rho'} \tag{47}$$

t' corresponds to ρ' according to (41), and

$$K(t, t') = \int_0^{\hat{k}_0}\left[j\frac{\left[nH_n^{(1)}(k_0t') - k_0t'H_{n-1}^{(1)}(k_0t')\right]H_n^{(1)}(k_0t')H_n^{(2)}(k_0t_a)}{H_n^{(1)}(k_0t_a)} \cdot J_0(k_0t)\right]k_0\,dk_0 \tag{48}$$

is a variable-resolution selective function with a maximum at $t' = \hat{t}(t)$. It can be used to sample $G(\tilde{\varepsilon}_r(t'))$ at $t' = \hat{t}$ according to

$$G\left[\tilde{\varepsilon}_r(\hat{t})\right] = \frac{\hat{r}\left[t(\hat{t})\right]}{\int_{t_a}^{t_0} K\left[t(\hat{t}), t'\right]\,dt'} \tag{49}$$

with $t(\hat{t})$ as the inverse function of $\hat{t}(t)$.

Finally, the unknown permittivity profile $\varepsilon_r(t)$ can be readily reconstructed as

$$\varepsilon_r(t) = \delta^2 + \left[\varepsilon_r(a) - \delta^2\right] * \exp\left[\frac{8}{\pi}\int_{t_a}^{t} G(\tilde{\varepsilon}_r(x))\,dx\right] \tag{50}$$

where $\varepsilon_r(a)$ is the permittivity at the outer air–dielectric interface and x is a dummy integration variable.

B. TM_{mn} Cylindrical Wave

For the inverse solution and reconstruction of the permittivity profile using TM_{mn} illumination, we start with (35) and follow exactly the same procedure and apply the similar kind of boundary condition as for the TE_{mn} case. The virtual reflection coefficient $\hat{\Gamma}(\rho)$ for this case is given by (51), shown at the bottom of this page.

Equation (51) is simplified making use of (41) and (43) to obtain the following:

$$\hat{\Gamma}(k_0, t_a) = \int_{t_a}^{t_0}\left\{\frac{\pi\left[2\tilde{\varepsilon}_r(\rho') - \varepsilon_r(\rho')\right]}{8\varepsilon_r(\rho')\tilde{\varepsilon}_r(\rho')\sqrt{\tilde{\varepsilon}_r(\rho')}}\frac{d\tilde{\varepsilon}_r(\rho')}{d\rho'} \cdot j\frac{\left[k_0t'H_{n-1}^{(1)}(k_0t') - nH_n^{(1)}(k_0t')\right]}{H_n^{(1)}(k_0t_a)} \cdot H_n^{(1)}(k_0t')H_n^{(2)}(k_0t_a)\right\}dt'. \tag{52}$$

Next, the truncated Hankel transform is introduced as in the TE case and the different terms in (46) are obtained as follows:

$$G(\tilde{\varepsilon}_r(t')) = \frac{\pi\left[2\tilde{\varepsilon}_r(\rho') - \varepsilon_r(\rho')\right]}{8\varepsilon_r(\rho')\tilde{\varepsilon}_r(\rho')\sqrt{\tilde{\varepsilon}_r(\rho')}}\frac{d\tilde{\varepsilon}_r(\rho')}{d\rho'} \tag{53}$$

$$K(t, t') = \int_0^{\hat{k}_0}\left[j\frac{\left[k_0t'H_{n-1}^{(1)}(k_0t') - nH_n^{(1)}(k_0t')\right]H_n^{(1)}(k_0t')H_n^{(2)}(k_0t_a)}{H_n^{(1)}(k_0t_a)} \cdot J_0(k_0t)\right]k_0\,dk_0. \tag{54}$$

Finally, the unknown permittivity profile $\varepsilon_r(t')$ is reconstructed as

$$\varepsilon_r(t) = \frac{[\varepsilon_r(a)]^2}{[\varepsilon_r(a) - \delta^2]} * \exp\left[\frac{8}{\pi}\int_{t_a}^{t} G(\tilde{\varepsilon}_r(x))\,dx\right] - \delta^2 \tag{55}$$

where all the symbols have the same meaning as in the TE_{mn} case.

C. Numerical Inversion Algorithm

The permittivity profile as being reconstructed according to (50) uses the virtual time variable t. To reconstruct the actual radially varying permittivity profile, we need to convert t into the space variable ρ. Thus, our concern is to find accurately the value of ρ', which corresponds to the particular value of t'. Below we present a simple numerical algorithm based on (41) and (50) for this purpose.

Let

$$g(t') = \left[\frac{8}{\pi}\int_{t'_a}^{t'} G(\tilde{\varepsilon}_r(x))\,dx\right]$$

$$\hat{\Gamma}(k_0, a) = \int_a^{\rho_0}\left\{\frac{j\pi\rho' k_0}{8\varepsilon_r(\rho')}\frac{2\tilde{\varepsilon}_r(\rho') - \varepsilon_r(\rho')}{\sqrt{\tilde{\varepsilon}_r(\rho')}}\frac{d\tilde{\varepsilon}_r(\rho')}{d\rho'}\left[H_{n-1}^{(1)}(k_{\rho'}\rho') - \frac{n}{k_{\rho'}\rho'}H_n^{(1)}(k_{\rho'}\rho')\right] \cdot H_n^{(2)}(k\rho') \cdot \exp\left[\int_a^{\rho'}\frac{4j}{\pi\rho''H_n^{(1)}(k_{\rho''}\rho'')H_n^{(2)}(k_{\rho''}\rho'')}\,d\rho''\right]\right\}d\rho' \tag{51}$$

then (50) becomes

$$\varepsilon_r(t') = \delta^2 + \left[\varepsilon_r(a) - \delta^2\right] * \exp\left[g(t')\right].$$

Starting with $g(t'_1) = g(t_a) = 0$, we follow the development of $g(t')$ in a very small time step $\Delta t'$

1) At $t' = t'_1 = t'_a = a\sqrt{\varepsilon_r(a)} = \rho'_1\sqrt{\varepsilon_r(t'_1)}$

$$\Rightarrow \rho'_1 = a \quad \varepsilon_r(t'_1) = \varepsilon_r(a).$$

2) In general, at $t' = t'_i = t'_{i-1} - \Delta t'$

$$g(t'_i) = \frac{-4\Delta t'}{\pi}\left[G(\varepsilon_r(t'_{i-1})) + G(\varepsilon_r(t'_i))\right]$$
$$\varepsilon_r(t'_i) = \delta^2 + \left[\varepsilon_r(a) - \delta^2\right] * \exp\left[g(t'_i)\right]$$

with

$$\Delta t' = t'_{i-1} - t'_i \cong (\rho'_{i-1} - \rho'_i)\left[\frac{\sqrt{\varepsilon_r(t'_{i-1})} + \sqrt{\varepsilon_r(t'_i)}}{2}\right]$$
$$\Rightarrow \rho'_i = \rho'_{i-1} - \frac{2\Delta t'}{\sqrt{\varepsilon_r(t'_{i-1})} + \sqrt{\varepsilon_r(t'_i)}}$$

where t'_i corresponds to ρ'_i according to (41).

As $\varepsilon_r(t'_i)$ is already determined at sampled intervals t'_i, $i = 2, 3, \ldots, N$ and the interval $\Delta t'$ is chosen to be very small, the exact value of ρ'_i corresponding to the particular value of t'_i can be very accurately determined in subsequent steps using the above algorithm.

The above algorithm is basically valid for a TE_{mn} illumination. The algorithm for the TM_{mn} case can, however, be developed using (41) and (55) exactly on similar lines as described above.

IV. Reconstructed Examples

Figs. 2 and 3 show the actual and reconstructed linearly varying permittivity profiles for a TE_{10} illumination for a quite high relative permittivity. As can be seen from (50) and (55), the reconstruction of the radially varying permittivity profile using a higher order TE illumination is simpler, as compared to that corresponding to a higher order TM illumination. It is also obvious from (39) that for the cylindrical objects having finite axial length, the radial propagation constant depends on the axial direction if it is not possible to excite the lowest order radial mode (TM_{00}). It is, therefore, always recommended to use a TE illumination when the cylindrical object has a finite length in the axial direction and the radial propagation constant can no longer be taken to be independent of the axial length. Another parameter, which is very critical for the reconstruction of the finite-length cylindrical object, is the lowest value of the normalized free-space wavenumber over which the measurement is carried out. Ideally, this value should vanish [see (45)]. However, since the Hankel functions are singular when their arguments approach zero, we thus skip this point and start from any finite value close to zero. Another possibility is to replace the Hankel functions by their small argument asymptotic expressions and to compute (48) and (49) analytically near the zero argument region. The selection of the lowest value of this free-space wavenumber, however, depends on two factors. If we take this value to be very low, then the parameter δ may be quite high and comparable with $\varepsilon_r(\rho)$, which may give some error in the calculation of the effective relative permittivity $\tilde{\varepsilon}_r(\rho)$ in (39). On the other hand, if we take this value to be quite high, then the reconstruction may not be accurate, as our inverse algorithm is quite sensitive to the lower values of k_0. Thus, a tradeoff has to be done to optimize this lower value of k_0.

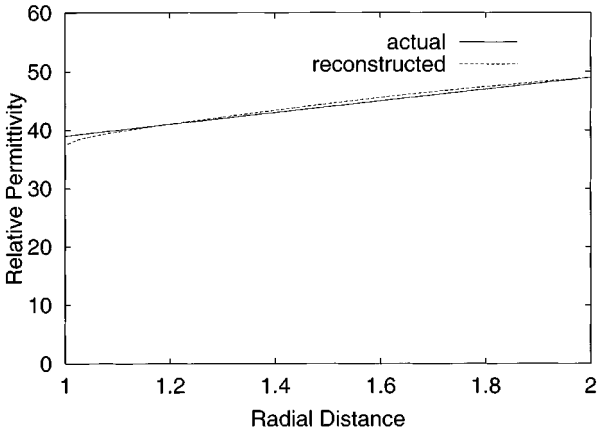

Fig. 2. Actual and reconstructed profiles for the linear case (TE mode).

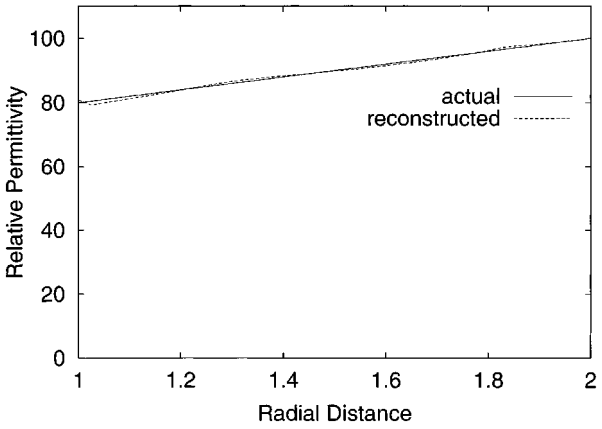

Fig. 3. Actual and reconstructed profiles for quite high value of permittivity (TE mode).

In Fig. 4, a TM_{10} illumination is considered for a case with a unity relative permittivity at the outer radius (i.e., same as that of free space). The object can be assumed infinitely long in the axial direction. It may be noted here that, for the cylindrical objects, which can be taken as infinitely long in the axial direction and where the radial propagation constant k_ρ can be approximated by the total propagation constant k, TM_{00} illumination is advantageous. This is because the TM_{00} mode is basically the transmission line one and, hence, the overall analysis can be greatly simplified. Fig. 5 shows the reconstruction of one more linearly varying profile using a TM_{01} illumination. As can be easily seen from all of the above linear profiles, there is an excellent agreement between the exact and reconstructed profiles for all the cases even when the relative permittivity is quite high.

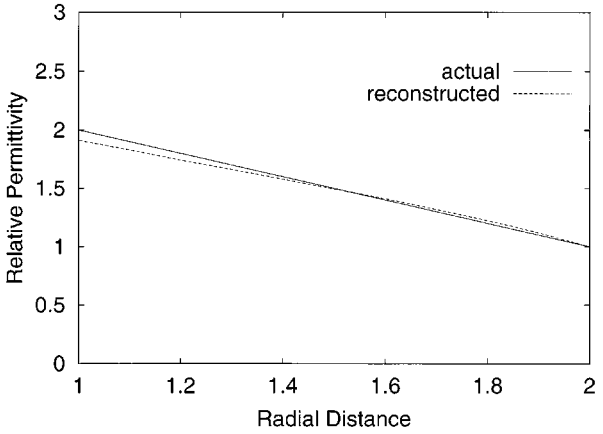

Fig. 4. Actual and reconstructed profiles with continuity at the air–dielectric interface (TM mode).

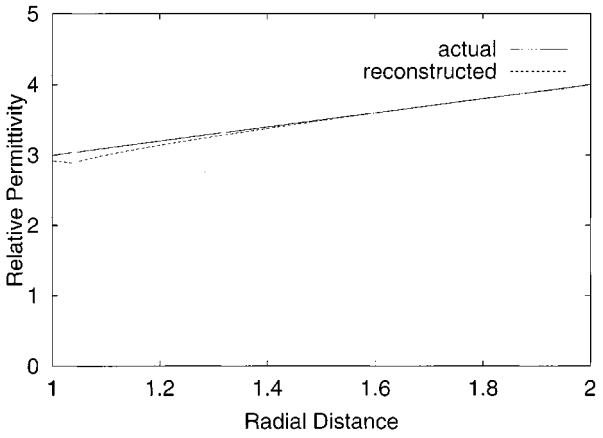

Fig. 5. Actual and reconstructed profiles for the linear case (TM mode).

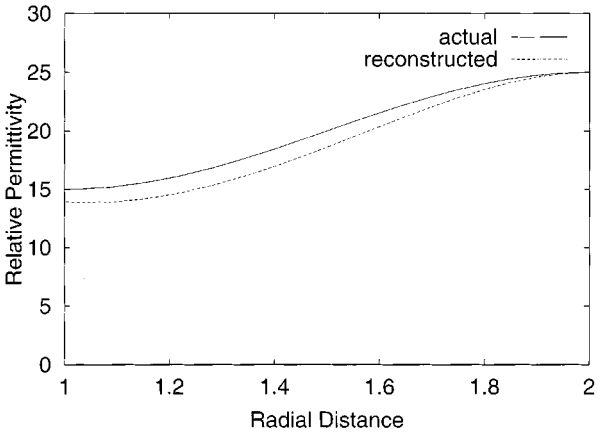

Fig. 6. Actual and reconstructed profiles for the nonlinear case (TM mode).

Fig. 6 shows the nonlinear profile considering a TM_{01} illumination. As evident from this plot, the agreement between the original and reconstructed profiles is not as good as it was for the linear case. This is because of the fact that the spatial derivative of the relative permittivity is reasonably high in this case. However, the agreement between the actual and reconstructed profiles is better even for the nonlinear case provided that the relative permittivity is also quite high. This is obvious from Fig. 7,

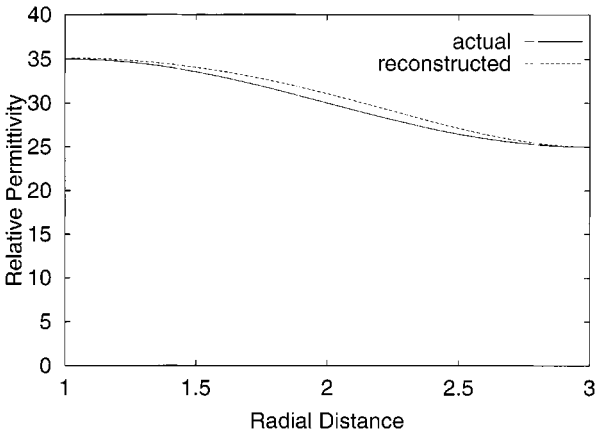

Fig. 7. Actual and reconstructed profiles for the nonlinear case (TM mode).

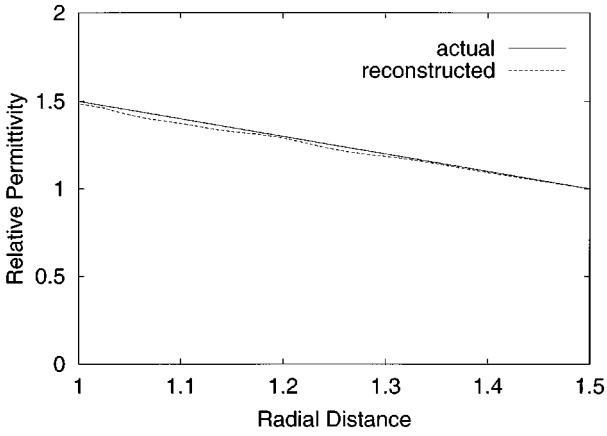

Fig. 8. Actual and reconstructed profiles with 5% random noise.

where, again, a TM_{01} illumination was used. This may be explained from (41) as in this case, the relative permittivity is high as compared to its spatial derivative and, hence, the second term on the right-hand side of this equation can be easily neglected. In all the above examples, error- and noise-free scattering data have been synthetically produced by solving the nonlinear Riccati-similar differential equations for known permittivity profiles using MATLAB.

In Fig. 8, the scattering data contains some random noise to comply with the actual measuring conditions. This is done by adding some random error to the calculated reflection coefficient data $\Gamma(k_0) + 0.05 * (\mathrm{RAND} - 0.5)$, where $\Gamma(k_0)$ is the calculated reflected coefficient and RAND is a uniformly distributed random number satisfying $0 \leq \mathrm{RAND} \leq 1$. As readily observed from this example, even with 5% random noise in the scattering data, there is a very good match between the actual and reconstructed profiles. It is worth noting here that the inverse problems are generally very ill poised and, thus, they are quite sensitive to the measuring data. Sometimes even a small change in the measuring data may result in very large deviation in the reconstructed parameter if any numerical methods are used. Thus, the ruggedness of our inverse algorithm to the input measuring data is also one of the main advantages of the method proposed here.

In all the above examples, around 100 to 150 data points covering the spectral wavelength range from infinity down to

one-fifth of the inner diameter of the cylindrical object have been used for the reconstruction of the profile using our proposed technique. The radial distance in the above plots has been normalized with respect to the inner radius of the cylindrical object under consideration. A number of other permittivity profiles have also been considered for the validation of our algorithm and a similar reconstruction accuracy behavior was observed in most of the cases.

V. Conclusion

A novel technique for the reconstruction of permittivity profiles in cylindrical geometries making use of a higher order mode illumination has been presented in this paper. Two nonlinear Riccati-similar differential equations for the TE_{mn} and TM_{mn} cylindrical modes have first been derived for this purpose. These equations have then been inverted using our proposed technique. The method proposed here gives a unique solution and can be used to reconstruct profiles with higher contrasts as well. Several linear as well as nonlinear profiles have been considered for the validation of our technique and, in each case, a very good agreement was found between original and reconstructed values. Finally, the effect of noise has been also considered and it was observed that the technique presented here is not very sensitive to the noise. This is especially advantageous in the real-time measuring condition, where a few percent error in the measurement data is unavoidable.

References

[1] M. O. Kolawole, "Scattering from dielectric cylinders having radially layered permittivity," *J. Electromag. Waves Applicat.*, vol. 6, no. 2, pp. 235–259, 1992.

[2] L. Tsang and J. A. Kong, "Application of strong fluctuation random medium theory to scattering from vegetation-like half space," *IEEE Trans. Geosci. Remote Sensing*, vol. GRS-19, pp. 62–69, Jan. 1981.

[3] J. J. Xia, T. M. Habashy, and J. A. Kong, "Profile inversion in a cylindrically stratified lossy medium," *Radio Sci.*, vol. 29, no. 4, pp. 1131–1141, July/Aug. 1994.

[4] A. Broquetas, J. Romeu, J. M. Rius, A. R. Elias-Fuste, A. Cardama, and L. Jofre, "Cylindrical geometry: A further step in active microwave tomography," *IEEE Trans. Microwave Theory Tech.*, vol. 39, pp. 836–844, May 1991.

[5] N. Joachimowicz, J. J. Mallorqui, J.-C. Bolomey, and A. Broquetas, "Convergence and stability assessment of Newton–Kantorovich reconstruction algorithm for microwave tomography," *IEEE Trans. Med. Imag.*, vol. 17, pp. 562–570, Aug. 1998.

[6] T. M. Habashy, W. C. Chew, and E. Y. Chow, "Simultaneous reconstruction of permittivity and conductivity profiles in a radially inhomogeneous slab," *Radio Sci.*, vol. 21, no. 4, pp. 635–645, Jul.-Aug. 1986.

[7] W. Tabarra, "Reconstruction of permittivity profiles from a spectral analysis of the reflection coefficient," *IEEE Trans. Antennas Propagat.*, vol. AP-27, pp. 241–244, Mar. 1979.

[8] A. K. Jordan and H. D. Ladouceur, "Renormalization of an inverse-scattering theory for discontinuous profiles," *Phys. Rev. A, Gen. Phys.*, vol. 36, no. 9, p. 4245, 1987.

[9] T. J. Cui and C. H. Liang, "Nonlinear differential equation for the reflection coefficient of an inhomogeneous lossy medium and its inverse scattering solutions," *IEEE Trans. Antennas Propagat.*, vol. 42, pp. 621–626, May 1994.

[10] M. J. Akhtar and A. S. Omar, "Reconstructing permittivity profiles using an improved renormalization technique," in *IEEE MTT-S Int. Microwave Symp. Dig.*, Anaheim, CA, June 1999, pp. 1815–1818.

[11] A. S. Omar and M. J. Akhtar, "A Hankel-transform reconstruction technique for radially dependent permittivity profiles in cylindrical objects," in *Proc. European Microwave Conf.*, Munich, Germany, Oct. 1999, paper WED4–4.

[12] R. F. Harrington, *Time-Harmonic Electromagnetic Fields*. New York: McGraw-Hill, 1961.

M. J. Akhtar (S'98) was born in Gaya, India, in March, 1971. He received the B.Sc. Engg. degree in electronics engineering from the Aligarh Muslim University, Aligarh, India, in 1990, the M.E. degree in electronics and communication engineering with specialization in microwave engineering from the Birla Institute of Technology, Ranchi, India, in 1993, and is currently working toward the Ph.D. degree in electrical engineering at the University of Magdeburg, Madgeburg, Germany. His doctoral research concerns the solution of electromagnetic inverse scattering problems and its application to the field of remote sensing and microwave imaging.

From 1993 to 1994, he was a Research Associate at the Central Electronics Engineering Research Institute, Pilani, India, and since 1994, has been a Scientist. His research interests include the design and development of microwave tubes, the optical control of microwave devices, and numerical techniques applied to the electromagnetic field problems.

Mr. Akhtar is a member of the Institution of Electronics and Telecommunication Engineers (IETE), India, the Indian Physics Association (IPA), and the Indo–French Technical Association (IFTA).

Abbas S. Omar (M'87–SM'89) received the B.Sc. and M.Sc. degrees from Ain Shams University, Cairo, Egypt, in 1978 and 1982, respectively, and the Doktor-Ing. degree in electrical engineering from the Technical University of Hamburg, Harburg–Hamburg, Germany, in 1986.

Since 1990, he has been Professor of electrical engineering and Head of Chair of microwave and communication engineering at the University of Magdeburg, Magdeburg, Germany. He authored or co-authored over 130 technical papers that extend across a wide spectrum of research areas. He recently directed his research activities to the solution of inverse problems related to remote sensing and microwave tomography. His current research fields cover the areas of remote sensing and microwave imaging, high-speed multimedia satellite and mobile communication, electromagnetic bullets and their applications to secure low-power wide-band communications and subsurface tomography, stochastical electromagnetics and their meteorological, environmental and biomedical applications, field theoretical modeling of microwave systems and components, microwave measurements, and submillimeter-wave signal generation and processing. He is an Editorial Board member of *Proceedings IEE, Electronics Letters*, and the *Journal of Electromagnetics*.

Dr. Omar is a member of the Technical Program Committee of IEEE Microwave Theory and Techniques Society (IEEE MTT-S) Symposium. He is an Editorial Board member of IEEE TRANSACTIONS ON MICROWAVE THEORY AND TECHNIQUES, the IEEE TRANSACTIONS ON ANTENNAS AND PROPAGATION, and the IEEE MICROWAVE AND GUIDED WAVE LETTERS. He is also the IEEE MTT-S Financial Coordinator for Region 8.